Simple model for the Bénard instability with horizontal flow near threshold

Helmut R. Brand
Fachbereich 7, Physik, Universität Essen, D43 Essen 1, Federal Republic of Germany
and Center for Nonlinear Studies, MS-B 258, Los Alamos National Laboratory, Los Alamos, New Mexico 87545

Robert J. Deissler
Center for Nonlinear Studies, MS-B 258, Los Alamos National Laboratory, Los Alamos, New Mexico 87545

Guenter Ahlers
Department of Physics and Center for Nonlinear Sciences, University of California, Santa Barbara, California 93106
and Center for Nonlinear Studies, MS-B 258, Los Alamos National Laboratory, Los Alamos, New Mexico 87545
(Received 28 November 1990)

We present a simple model for Rayleigh-Bénard convection with an imposed horizontal flow of Reynolds number R in a container of finite width and near threshold. The model consists of two coupled envelope equations representing longitudinal and transverse traveling convection rolls. Each equation is for a wave traveling in the direction of the imposed flow. For small R, transverse rolls are stable at the convective onset. For $R > R^*$, longitudinal rolls bifurcate from the conduction state. For a range of cross-coupling strengths and for $R > R^*$, we obtain a transition from longitudinal to transverse rolls as the Rayleigh number is increased. This transition occurs via states for which part of the system is occupied by longitudinal, and another by transverse rolls. The behavior is strongly influenced by the presence of noise since the system first becomes *convectively* unstable, and therefore noise-sustained structures can play an important role. We also show that for a range of parameters in the model, a mixed state (for which both envelopes assume a nonzero value at the same location) is possible over part of the cell in a finite geometry.

I. INTRODUCTION

During the last decade or so, experimental physicists interested in nonequilibrium systems have placed great emphasis[1] on the study of Rayleigh-Bénard convection[2,3] (RBC) and Taylor vortex flow[4,5] (TVF) in an attempt to understand the formation of patterns and the evolution of spatiotemporal chaos. This has been so because these systems can be quantitatively controlled in the laboratory. Although much has been learned from this work, these systems differ qualitatively from the large class of practically relevant *open* systems, such as shear, pipe, and channel flows, for which there is a mean externally imposed flow. Both RBC and TVF can be modified readily so as to add the major features of the open systems by imposing a horizontal flow in the former and an axial flow in the latter case. In practice, these modifications are possible without sacrificing the accurate control of boundary conditions and stress parameters which have been the hallmark of these two systems.

In the present paper, we concentrate on RBC with horizontal flow. Relatively little experimental work seems to have been done on this problem,[6-11] and the theoretical analysis[6,7,9,12,13] is also incomplete at this time. Here we discuss the structure, and the nature of the solutions, of a pair of coupled envelope equations for RBC with horizontal flow which we expect to be relevant to the real system in the weakly nonlinear region close to the first bifurcation. As did the work of Müller *et al.*,[13] these equations incorporate the shift of the bifurcation point of transverse rolls due to the flow, and contain the *convective* nature of the instability at the first bifurcation and the *absolute* instability at larger Rayleigh numbers. However, in addition, they also describe the effect of the flow upon the competition between transverse and longitudinal convection rolls which occurs in a finite container.

In a Rayleigh-Bénard cell, which is long and not too wide, rolls are expected to align parallel to the short side at the convective onset if there is no horizontal flow.[14] This prediction has been confirmed experimentally in several laboratories.[15-17] We call this alignment transverse rolls (TR). On the other hand, it is known from theory[18] that the convection rolls in a laterally infinite system align longitudinally, i.e., with the roll axes parallel to the flow (LR). In the finite laboratory system with flow parallel to the long side of the container, TR traveling in the downstream direction are found at the convective onset when the flow rates are small,[7,9-11] and LR become stable at onset for larger rates.[9-11] The range of stability of TR depends on the width of the container. The wider the cell, the smaller the range of flow rates over which they are stable. *Above* onset, a transition may occur also in certain parameter ranges between LR and TR as the Reynolds and/or Rayleigh numbers are varied. This transition can take place over a parameter range via states for which both LR and TR exist,[10,11] albeit in different parts of the cell. Very recently, it has been ob-

served experimentally that this transition is hysteretic.[10] In addition the stable coexistence of LR and TR at different spatial locations, a stable *superposition* of LR and TR at the *same* spatial location was also found in the experiments[10] for a small range of Reynolds and Rayleigh numbers.

From the theoretical point of view, most investigations have been focusing on the determination of the onset values of LR and TR,[6,7,9,12] and it has been found, in qualitative agreement with experiments, that TR are stable at low rates and are replaced by LR as the Reynolds number R is increased.[6,7,9] Recently,[13] an envelope equation valid in the weakly nonlinear range near the onset of TR was derived. It was pointed out[13] that the first instability is a *convective* instability, and that the question of whether a pattern becomes absolutely or convectively unstable[19–23] is important in the present connection. These results have been complemented by two-dimensional integrations of the Navier-Stokes equations for TR, and by the evaluation of the coefficients entering the envelope equation for TR.[13] In the present paper we give a simple model consisting of two envelope equations, one each for traveling transverse and longitudinal rolls.

II. MODEL

To keep the model as simple as possible, we consider slow spatial variations in the flow direction only. In addition, we assume, consistent with all available experimental evidence, that the first bifurcation remains forward (nonhysteretic) even in the presence of the horizontal flow. For that case, we get saturation to cubic order near threshold. Using the methods of Newell *et al.*,[24–28] we write the dynamic equations for slowly varying envelopes of LR and TR. Denoting the envelopes by A^L and A^T, respectively, we have

$$\tau_0^L(A_t^L+v^L A_x^L)=\chi^L A^L+\gamma^L A_{xx}^L -\beta^L|A^L|^2 A^L-\delta^L|A^T|^2 A^L \quad (1a)$$

and

$$\tau_0^T(A_t^T+v^T A_x^T)=\chi^T A^T+\gamma^T A_{xx}^T -\beta^T|A^T|^2 A^T-\delta^T|A^L|^2 A^T . \quad (1b)$$

Although for $R=0$, the lowest-order gradient term in the equation for A^L would be A_{xxxx},[29] the anisotropy introduced by the flow leads to a second-order gradient term. Since this term is of lower order than the A_{xxxx} term, we have neglected the latter. Although the fourth-order term would become important as R goes to zero, it turns out that the longitudinal mode does not have a finite amplitude at small R. Thus the details of Eq. (1a) become irrelevant to our model in that limit. We note that for the onset of LR or TR the horizontal flow introduces a preferred direction into the system and that there are no rolls which travel in the upstream direction. Therefore, only rolls traveling in the positive direction are contained in Eqs. (1a) and (1b). The coefficients γ^L, γ^T, β^L, β^T, δ^L, and δ^T are complex and of the form $\alpha=\alpha_r+i\alpha_i$.

III. PARAMETERS AND BIFURCATIONS

The coefficients τ_0^T, v^T, γ_r^T, γ_i^T, β_r^T, and β_i^T have been determined in Ref. 13 for a system of infinite extent in the direction perpendicular to the flow. We define $\chi^L=\epsilon-\epsilon_1$ and $\chi^T=\epsilon-\epsilon_3$, with $\epsilon=R_a/R_a^c-1$ and R_a^c equal to the critical Rayleigh number[14] without flow. Values for ϵ_1 and ϵ_3 have been given in Ref. 6 as a function of the Reynolds number R of the horizontal flow. For illustrative purposes, we consider in the present paper the particular example where the width of the cell is equal to twice the height and where the Prandtl number is equal to 7. For that case the results of Ref. 6 can be represented by

$$\epsilon_1=0.0504 \quad (2a)$$

and

$$\epsilon_3=0.0227R^2-0.000\,136R^4 . \quad (2b)$$

The corresponding bifurcation lines are shown in Fig. 1 as the curves labeled 1 and 3. We identify the value of R at which they cross as R^*. For the remaining coefficients of Eqs. (1a) and (1b) no data seem to be available in the literature. It was found in Ref. 13 that the imaginary parts of the coefficients for the TR are very small. The same can be expected to hold for these coefficients in the equation for the LR. Indeed, there are no indications in the experimental results[7–11] that significant effects come

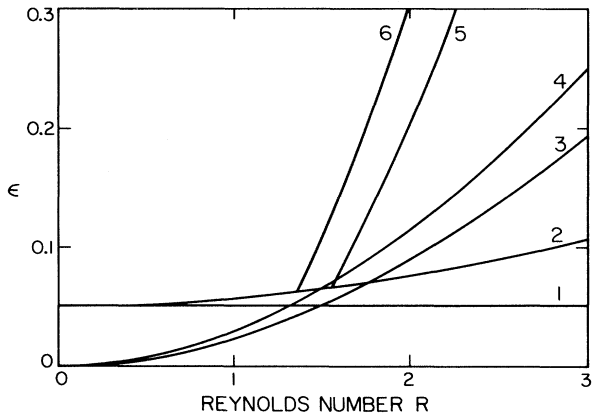

FIG. 1. Instability lines for transverse and longitudinal rolls as a function of the Reynolds number R. Above these lines the system is unstable for the corresponding type of instability and rolls pattern: at curve 1 the zero-amplitude state becomes convectively unstable to longitudinal rolls; at curve 2 the zero-amplitude state becomes absolutely unstable to longitudinal rolls; at curve 3 the zero-amplitude state becomes convectively unstable to transverse rolls; and at curve 4 the zero-amplitude state becomes absolutely unstable to transverse rolls. Curves 1–4 are associated with linear properties only. Lines 5 and 6 incorporate the influence of the cross coupling between longitudinal and transverse rolls on the instability lines as they arise for the parameter values considered in the bulk part of this manuscript. At curve 5 saturated longitudinal rolls become convectively unstable to transverse rolls, and at curve 6 saturated longitudinal rolls become absolutely unstable to transverse rolls.

from the imaginary parts. We have taken all coefficients to be real in most of the numerical runs presented below, and have done some computations with small values of the imaginary coefficients to check that these do no introduce any qualitative differences. For our illustrative purposes, we have also used $v^T=v^L=R$ and $\tau_0^T=\tau_0^L=0.05$. The former is roughly consistent with the result of Ref. 13 for TR, and the latter is typical of the value of τ_0 for RBC without flow.[30] In addition, we chose the coefficients of the diffusive terms γ_r^L and γ_r^T equal to 0.1, which is of the same magnitude as the value of γ^T for RBC without flow.[30] We would expect γ_r^L to vanish as R goes to zero; but, as we will see, this mode does not have a finite amplitude for small R and thus the behavior of the coefficient as R vanishes is irrelevant. Our choice $\gamma_r^L=0.1$ is arbitrary, and we use it for illustrative purposes only. We set the cubic coefficients β_r^L and β_r^T equal to 1.0. This choice does not influence the results, since these coefficients can be changed at will by rescaling both amplitudes separately.

The choice of the cross-coupling coefficients has a substantial effect on the patterns predicted by the equations. In order to produce examples of some of the states seen in the experiments,[10,11] we chose $\delta_r^T=0.75$ and $\delta_r^L=1.5$. Most of the numerical work described below has been done with these parameters. The thresholds ϵ_1 and ϵ_3 calculated from the linearized stability analysis[6] correspond to the onset of a convectively unstable state for which perturbations viewed at a fixed location decay, whereas in a moving frame they grow. The onset of an absolutely unstable state, in which perturbations viewed at a fixed location grow, is shifted to higher values of ϵ. For the case of the envelope equation with complex coefficients for waves traveling in one direction, this upward shift has been shown[20–22] to be $(v^2\tau_0^2\gamma_r)/(4|\gamma|^2)$. Thus, with γ^T and γ^L real, we obtain the two additional bifurcation lines

$$\epsilon_2=\epsilon_1+(v^L\tau_0^L)^2/4\gamma^L \tag{3a}$$

and

$$\epsilon_4=\epsilon_3+(v^T\tau_0^T)^2/4\gamma^T . \tag{3b}$$

These results are shown in Fig. 1 by the lines labeled 2 and 4.

The curves 1–4 in Fig. 1 are relevant only when the pair of bifurcations (convective and absolute) is the first pair of instabilities as ϵ is increased. They are modified for the second pair by the finite amplitude of the first because of the cross coupling in Eqs. (1a) and (1b).[23]. Thus, for $R>R^*$, where LR appear first, the effective growth rate for a TR [see Eq. (1b)] is proportional to $\chi^T-\delta_r^T|A^L|^2$, and both the convective and absolute instability for the TR will be shifted upward. Therefore, we plotted in Fig. 1 as curves 5 and 6 the convective and absolute instability lines, respectively, for the TR, assuming that the LR have reached their saturated amplitude. The corresponding equations for real coefficients are

$$\epsilon_5=(\epsilon_3-\delta^T\epsilon_1/\beta^L)/(1-\delta^T/\beta^L) \tag{4a}$$

and

$$\epsilon_6=\epsilon_5+(v^T\tau_0^T)^2/[4\gamma^T(1-\delta^T/\beta^L)] . \tag{4b}$$

Equation (4a) was found by setting the effective growth rate for TR in the presence of LR to zero and solving for ϵ. Here we have used $|A^L|^2=\chi^L/\beta_r^L$. Equations (4a) and (4b) permit a positive growth rate only for $\delta_r^T/\beta_r^L<1$. For $\delta_r^T/\beta_r^L>1$, transverse rolls will not occur above R^* for any value of ϵ. We note that our curve 5 or 6 qualitatively reproduces the rapid rise of the corresponding experimental boundary between region III and IV in Fig. 18 of Ref. 10. A detailed comparison of these boundaries with quantitative experiments could yield realistic values of the coupling coefficients. Similarly, for $R<R^*$, where TR grow first, the effective growth rate of LR is proportional to $\chi^L-\delta_r^L|A^T|^2$. For the parameters used in most of our numerical calculations, $\delta_r^L/\beta_r^T>1$, and the cross coupling leads to a negative growth rate for the longitudinal rolls at all values of ϵ. Therefore, for our example, no further bifurcation lines appear in Fig. 1; but for $\delta_r^L/\beta_r^T<1$, a transition with increasing ϵ from TR to LR would exist for $R<R^*$. The corresponding equations for real coefficients are

$$\epsilon_7=(\epsilon_1-\delta^L\epsilon_3/\beta^T)/(1-\delta^L/\beta^T) \tag{5a}$$

and

$$\epsilon_8=\epsilon_7+(v^L\tau_0^L)^2/[4\gamma^L(1-\delta^L/\beta^T)] . \tag{5b}$$

IV. NONLINEAR STATES

In the following we report the results of our investigations of the patterns predicted by Eqs. (1a) and (1b). Since not all coefficients of Eqs. (1a) and (1b) are known for the system of interest, our aim is primarily to explore the qualitative features of the predicted patterns. A quantitative comparison will have to await the theoretical calculations or experimental determination of the relevant parameters. For the spatially uniform, time-independent states, it is easy to show for real coefficients that

$$|A^T|^2=\frac{\chi^T/\delta^T-\chi^L/\beta^L}{\beta^T/\delta^T-\delta^L/\beta^L} \tag{6a}$$

and

$$|A^L|^2=\frac{\chi^L/\delta^L-\chi^T/\beta^T}{\beta^L/\delta^L-\delta^T/\beta^T} . \tag{6b}$$

These equations apply only if $|A^L|^2$ and $|A^T|^2$ are positive. These simple analytical results suggest that mixed states, with finite amplitudes for both types of rolls, should exist in this model for certain parameter ranges. In order to explore the model with spatial variation, we proceed numerically. Except when otherwise noted, we used the parameter values discussed above. We usually applied Gaussian noise of standard deviation σ to both amplitudes at the left boundary of the container, thus stimulating experimental noise contained in the inflow.

In order to check whether the pattern observed is due to noise or whether the system is absolutely unstable, we sometimes reduced the noise strength to zero. An absolutely unstable pattern should change very little when the noise is removed, whereas the pattern should disappear altogether at zero noise level if the system is convectively unstable. In Fig. 2 we show results for $R=2>R^*$. The longitudinal rolls gradually fill in as ϵ is increased from 0.0625 to 0.08. This run was done for a noise strength $\sigma=10^{-5}$. For $\epsilon=0.08$, removal of the noise had almost no effect upon the pattern, showing that this ϵ value is above the absolute instability. For the patterns shown in Figs. 2(a) and 2(b) the pattern moved out of the system in the downstream direction when the noise was removed, and thus these patterns represent a noise-sustained structure, i.e., a pattern that is only stable in the presence of noise.[20–23] These results are consistent with the bifurcation lines given in Fig. 1.

It will be most interesting to see whether some of the patterns observed in experiments are also noise sustained. This could be explored by deliberately increasing the noise strength near the inflow boundary. Then the prediction for a noise-sustained structure would be that the pattern moves upstream, taking up a larger fraction of the cell. The portion of the cell in which the amplitude remains small should vary linearly with the logarithm of the noise intensity.[21] Another way of exploring this issue is to make quantitative determinations of the spatial evolution in the downstream direction of the pattern amplitude at constant noise level, but as a function of ϵ. The dependence of this evolution upon $\epsilon-\epsilon_2$ or $\epsilon-\epsilon_4$ in the noise-free system differs considerably from the corresponding dependence upon $\epsilon-\epsilon_1$ or $\epsilon-\epsilon_3$ in the noisy system. In the latter case, the amplitude grows initially with a characteristic length given by[20,21]

$$l_{\rm stoc}^{-1}=\frac{\gamma_r}{2|\gamma|^2}\left[v\tau_0-\left[v^2\tau_0^2-4\chi\frac{|\gamma|^2}{\gamma_r}\right]^{1/2}\right], \tag{7}$$

where we omitted the superscript L or T because the same equation applies to both modes. In the deterministic case above the absolute instability, the ϵ dependence of the corresponding length is known only numerically,[13] but seems to differ substantially from that given by Eq. (7).

For $R>R^*$, a further increase of ϵ can lead to transverse rolls only for ϵ values above curve 5 in Fig. 1. In Fig. 3 we show what happens for $R=2$ as the value of ϵ is increased from $\epsilon=0.23$, where one has only longitudinal rolls, to $\epsilon=0.265$. With increasing ϵ, the fraction of the cell filled with transverse rolls increases. The TR fill in from the downstream end of the container, in agreement with recent experimental observations.[11] In the part of the system occupied by the TR, the LR are suppressed due to the presence of the cross coupling in Eq. (1a). If the value of ϵ is gradually decreased after a pure transverse state has been reached at large ϵ, we find that the pure transverse state is stable down to a value of $\epsilon=0.235$, showing that there is hysteresis with increasing and decreasing ϵ. However, if ϵ is never increased sufficiently far to reach the pure transverse state, then there is no hysteresis upon decreasing ϵ. These results show that the effective threshold values plotted as curves 5 and 6 in Fig. 1 determine which patterns are going to be observed, and not the linearized results shown as curves 3 and 4. When hysteresis exists, then, upon decreasing ϵ to 0.235, the TR are gradually replaced as a function of time by the LR. This once more shows the

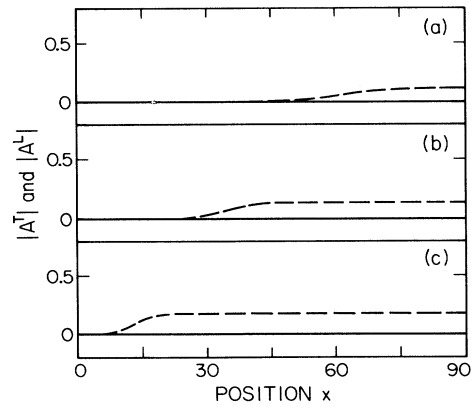

FIG. 2. Flow patterns for fixed Reynolds number $R=2$ and fixed noise level $\sigma=10^{-5}$ as a function of ϵ. Solid lines: the modulus of the amplitudes of the transverse rolls (TR). Dashed lines: the modulus of the amplitudes of the longitudinal rolls (LR). The data are in the vicinity of the absolute instability of the zero-amplitude state to longitudinal rolls. (a) $\epsilon=0.0625$, convectively unstable (noise-sustained structure); (b) $\epsilon=0.07$, convectively unstable (noise-sustained structure); (c) $\epsilon=0.08$, absolutely unstable.

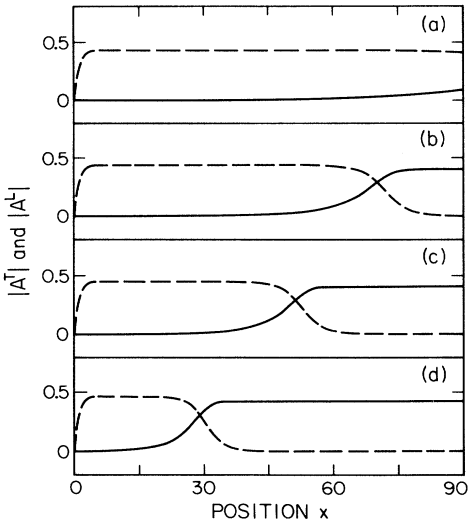

FIG. 3. Patterns for fixed Reynolds number $R=2$ and fixed noise level $\sigma=10^{-5}$ as a function of ϵ. Solid lines: the modulus of the amplitudes of TR. Dashed lines: the modulus of the amplitudes of the LR. The transverse rolls are noise-sustained structures. (a) $\epsilon=0.23$; (b) $\epsilon=0.24$; (c) $\epsilon=0.25$; (d) $\epsilon=0.265$.

importance of the cross-coupling terms in Eqs. (1a) and (1b). The present system is a particularly simple example of coexistence of and competition between two different types of patterns. We note that the hysteresis, and the coexistence of different patterns in different parts of the sample, have a strong similarity with regime IV given in Fig. 18 of Ref. 10.

To check whether our model contains also the direct transition to transverse rolls observed numerically and experimentally at small R, we performed the same simulations at the lower Reynolds number $R=1.5$. In Fig. 4 we show the resulting fully developed transverse roll pattern for $\epsilon=0.2$ under otherwise identical conditions and for the same choice of parameters as in Fig. 3. In this case, there are only transverse rolls, and indeed we found only transverse rolls up to $\epsilon=1.0$ in the present model. If this should be different in the experiment, this would give a good clue how to improve the model far above threshold in a regime where envelope equations are no longer expected to be applicable.

To see how a different noise strength influences the pattern observed under otherwise identical conditions, we have investigated the case arising for $R=2$ and $\epsilon=0.255$ for three different values of σ. From the results plotted in Fig. 5 we can clearly infer that the position of the interface separating longitudinal and transverse rolls depends on σ under otherwise identical conditions: the higher the noise strength, the higher the fraction of transverse rolls. As expected,[21] the length of the portion of the cell with small amplitude varies linearly with $\ln(\sigma)$.

In order to check whether the patterns depend on the path taken in the ϵ-R plane, we investigated the evolution of the pattern for fixed values of σ and ϵ as a function of R. The results are shown in Fig. 6. As in the case where ϵ was varied at constant R, we observed hysteresis, again showing the importance of the nonlinear cross-coupling terms. The magnitude of the hysteresis in R was about 5% for our parameter values.

All runs described so far were performed for the same values of the cross-coupling coefficients. They yielded coexistence of the two patterns in the same system, but at *different* spatial locations. An interesting issue is whether it is possible also to have the analogue of a mixed state,[28,31] that is of a state for which one has two envelopes coexisting at the *same* location, when other values of the coupling coefficients are used. We explored different values of the coupling terms and found that a mixed state does occur, and that its existence depends sensitively on the values of the coupling coefficients. In Fig. 7 we plotted a state for which one has longitudinal rolls existing alone near the inflow, but a well-pronounced mixed state in the downstream half of the container. It turns out that the ratio between the two envelopes in the mixed state can easily be inverted by changing one of the cross couplings by a few percent. To our knowledge, mixed states have not been examined before for spatially inhomogeneous situations. Equations

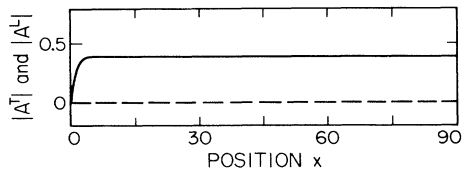

FIG. 4. Flow pattern for the smaller fixed Reynolds number $R=1.5$ for the same noise level as in Fig. 2 at $\epsilon=0.2$. Only transverse rolls are present.

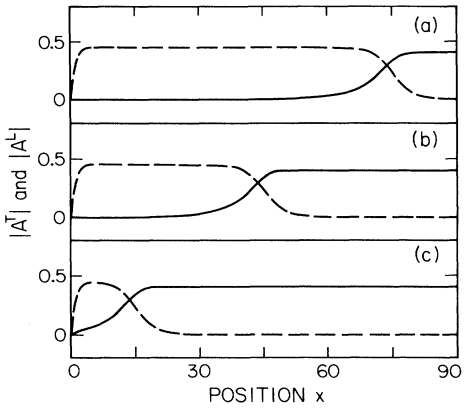

FIG. 5. Flow pattern for fixed Reynolds number $R=2$, fixed $\epsilon=0.255$, and variable noise level σ. Solid lines: the modulus of the amplitudes of the TR. Dashed lines: the modulus of the amplitudes of the LR. The transverse-roll patterns are noise-sustained structures. The larger the noise level, the larger the fraction of transverse rolls. (a) $\sigma=10^{-7}$; (b) $\sigma=10^{-5}$; (c) $\sigma=10^{-3}$.

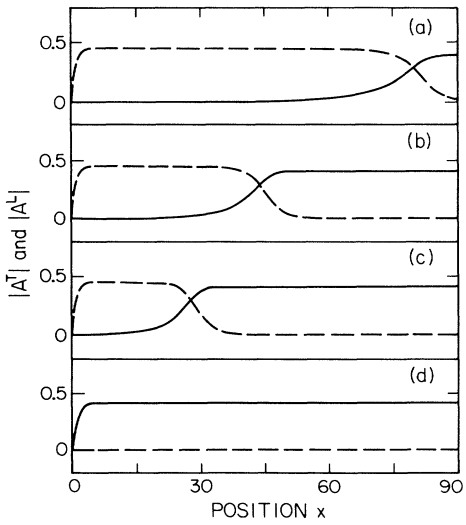

FIG. 6. Flow pattern for fixed noise level $\sigma=10^{-5}$ and fixed $\epsilon=0.255$ as a function of Reynolds number R. Solid lines: the modulus of the amplitudes of TR. Dashed lines: the modulus of the amplitudes of the LR. The transverse-roll patterns in (a), (b), and (c) are noise-sustained structures. (a) $R=2.05$; (b) $R=2.0$; (c) $R=1.975$; (d) $R=1.95$.

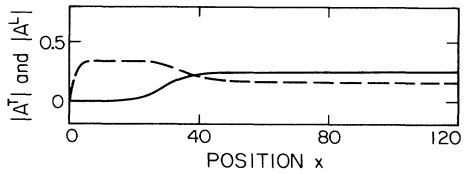

FIG. 7. Mixed pattern as it arises for slightly different values of the cross-coupling coefficients between longitudinal and transverse rolls. Solid line: the modulus of the amplitudes of TR. Dashed line: the modulus of the amplitudes of LR. For this example $\delta_r^T=0.5$, $\delta_r^L=1.4$, $\epsilon=0.165$, $R=2$, and $\sigma=10^{-5}$.

(1a) and (1b) provide a particularly simple model for this phenomenon. It seems likely that state V in Fig. 18 of Ref. 10 has common features with the mixed state shown in Fig. 7.

We want to emphasize that both the coexisting LR and TR and the mixed states described here are qualitatively different from the various types of confined states observed recently in binary fluid convection near the oscillatory onset.[32,33] In the latter case, one has a coexistence of amplitude zero over part of the cell with a finite amplitude over the remainder, and this phenomenon is linked to an inverted bifurcation. In the present case, we have investigated a model in which both the bifurcations to longitudinal and to transverse rolls are forward. In this case, the nonlinear cross couplings are responsible for the variety of states which exist.

V. SUMMARY

In the present paper we have shown that a simple model consisting of two envelope equations with slow spatial variations in one direction can reproduce the observed[10,11] spatially inhomogeneous states with different patterns in different parts of an experimental cell. For a certain parameter range, we have also found coexistence of two amplitudes at the same spatial location. We expect the model to be applicable to the Rayleigh-Benard system with an externally imposed horizontal flow. This system is a good candidate for the investigation of convectively unstable longitudinal- and transverse-roll patterns near threshold, and of the competition between these patterns above threshold. The addition of noise at the inlet, as well as the measurement of the amplitude profile as a function of ϵ, could show whether the experimentally observed[10,11] long influence length is indicative of noise-sustained structures. It will also be important to check, for example, by varying the width of the convective cell, whether it is possible to get a mixed state in this system which consists of a superposition of longitudinal and transverse rolls. Furthermore, it would be very interesting to study the hysteresis effects found in the model by quantitative experimental flow visualization of the entire cell.

Several of the results presented here can be expected to carry over to the case of thermal convection in a tilted cell.[34,35] In that case one also observes—as a function of tilt angle—a transition from transverse to longitudinal rolls. It should be kept in mind, however, that one has the superposition of a large convective roll and of the TR or LR, which makes the analysis more complicated than for RBC with horizontal flow and for the simple model presented here. We close by pointing out that some of the phenomena discussed here are also useful for Taylor-vortex flow with axial flow. The equations applicable in that case are, however, only uniaxial on length scales large compared to the pitch of the spiral flow-state which forms in that system.

ACKNOWLEDGMENTS

It is a pleasure to thank Steven Trainoff for sharing with us his experimental results prior to publication. We wish to thank Eberhard Bodenschatz and Hanns Walter Müller for illuminating conversations. G. A. acknowledges support through Department of Energy Grant No. DE-FG03-87ER13738 and through National Science Foundation Grant No. DMR88-14485. H.R.B. thanks the Deutsche Forschungsgemeinschaft for support. The work done at the Center for Nonlinear Studies, Los Alamos National Laboratory was performed under the auspices of the United States Department of Energy.

[1]See, for instance, in *Propagation in Systems Far From Equilibrium,* edited by J. E. Wesfreid, H. R. Brand, P. Manneville, G. Albinet, and N. Boccara, Springer Series in Synergetics Vol. 41 (Springer, New York, 1988); and G. Ahlers, in *Lectures on the Sciences of Complexity,* SFI Studies in the Sciences of Complexity, edited by D. Stein (Addison-Wesley, Reading, MA 1989), Vol. I, p. 175.

[2]H. Bénard, Rev. Gen. Sci. Pure Appl. **11**, 1261 (1900) **11**, 1309 (1900); Ann. Chim. Phys. **23**, 62 (1901); Lord Rayleigh, Philos. Mag. **32**, 529 (1916).

[3]A large literature pertaining to this field has evolved. Particularly useful as introductions to early work are the reviews by E. L. Koschmieder, Adv. Chem. Phys. **26**, 177 (1974); and in *Order and Fluctuations in Equilibrium and Nonequilibrium Statistical Mechanics,* XVIIth International Solvay Conference, edited by G. Nicolis, G. Dewel, and J. W. Turner (Wiley, New York, 1981), p. 168; and by F. Busse, in *Hydrodynamic Instabilities and the Transition to Turbulence,* edited by H. L. Swinney and J. P. Gollub (Springer, Berlin, 1984), p. 97; and in Rep. Prog. Phys. **41**, 1929 (1978).

[4]G. I. Taylor, Philos. Trans. R. Soc. London Ser. A **223**, 289 (1923).

[5]A sizable literature now exists dealing with this system. A comprehensive review has been given by R. C. DiPrima and H. L. Swinney, in *Hydrodynamic Instabilities and Transitions to Turbulence,* edited by H. L. Swinney and J. P. Gollub (Springer, Berlin, 1981). Important early papers in this field are numerous, but particularly noteworthy are D. Coles, J. Fluid Mech. **21**, 385 (1965); H. A. Snyder, J. Fluid Mech. **35**, 273 (1969); and J. E. Burkhalter and E. L. Koschmieder, Phys. Fluids **17**, 1929 (1974).

[6]J. K. Platten and J. C. Legros, *Convection in Liquids* (Springer,

New York, 1984), Chap. VIII.
[7]J. M. Luijkx, J. K. Platten, and J. C. Legros, Int. J. Heat Mass Transfer **24**, 1287 (1981).
[8]A. Pocheau, V. Croquette, P. LeGal, and C. Poitou, Europhys. Lett. **3**, 915 (1987).
[9]M. T. Ouazzani, J. P. Caltagirone, G. Meyer, and A. Mojtabi, Int. J. Heat Mass Transfer **32**, 261 (1989).
[10]M. T. Ouazzani, J. K. Platten, and A. Mojtabi, Int. J. Heat Mass Transfer **33**, 1417 (1990).
[11]S. Trainoff, G. Ahlers, and D. S. Cannell (private communication).
[12]J. M. Luijkx and J. K. Platten, J. Non-Equilib. Thermodyn. **6**, 141 (1981).
[13]H. W. Müller, M. Lücke, and M. Kamps, Europhys. Lett. **10**, 451 (1989).
[14]S. H. Davis, J. Fluid Mech. **30**, 465 (1967).
[15]K. Stork and V. Müller, J. Fluid Mech. **54**, 599 (1972).
[16]P. Kolodner, R. W. Walden, A. Passner, and C. M. Surko, J. Fluid Mech. **163**, 195 (1986).
[17]G. Ahlers and I. Rehberg, Phys. Rev. Lett. **56**, 1373 (1986); G. Ahlers, D. S. Cannell, and R. Heinrichs, Nucl. Phys. B (Proc. Suppl.) **2**, 77 (1987).
[18]For a review, see R. E. Kelly, in *Physiochemical Hydrodynamics,* edited by D. B. Spalding (Advanced, London, England, 1977), p. 65.
[19]P. Huerre, in *Instabilities and Nonequilibrium Structures,* edited by E. Tirapegui (Reidel, Dordrecht, 1987), p. 141.
[20]R. J. Deissler, J. Stat. Phys. **40**, 371 (1985).
[21]R. J. Deissler, Physica D **25**, 233 (1987).
[22]R. J. Deissler, J. Stat. Phys. **54**, 1459 (1989).
[23]R. J. Deissler and H. R. Brand, Phys. Lett. A **130**, 293 (1988).
[24]A. C. Newell, in *Lectures in Applied Mathematics,* edited by A. C. Newell (American Mathematical Society, Providence, RI, 1974), p. 157.
[25]A. C. Newell, in Ref. 1.
[26]H. R. Brand, P. S. Lomdahl, and A. C. Newell, Phys. Lett. A **118**, 67 (1986).
[27]H. R. Brand, P. S. Lomdahl, and A. C. Newell, Physica D **23**, 345 (1986).
[28]H. R. Brand and B. J. A. Zielinska, Phys. Rev. Lett. **57**, 3167 (1986).
[29]A. C. Newell and J. A. Whitehead, J. Fluid Mech. **38**, 279 (1969); L. A. Segel, *ibid.* **38**, 203 (1969).
[30]M. A. Dominguez-Lerma, G. Ahlers, and D. S. Cannell, Phys. Fluids **27**, 856 (1984); R. P. Behringer and G. Ahlers, Phys. Lett. **62A**, 329 (1977).
[31]B. J. A. Zielinska, D. Mukamel, and V. Steinberg, Phys. Rev. A **33**, 1454 (1986).
[32]P. Kolodner, D. Bensimon, and C. M. Surko, Phys. Rev. Lett. **60**, 1723 (1988).
[33]J. J. Niemela, G. Ahlers, and D. S. Cannell, Bull. Am. Phys. Soc. **33**, 2261 (1988); Phys. Rev. Lett. **64**, 1365 (1990).
[34]H. Ozoe, H. Sayama, and S. W. Churchill, Int. J. Heat Mass Transfer **20**, 123 (1977).
[35]O. Viett, Thèse de troisième cycle, Université Pierre et Marie Curie, Paris (unpublished); and O. Viett and J. E. Wesfreid (unpublished).